Predictions of a Spiral Diffusion Path for Nonspherical Organic Molecules in Carbon Nanotubes

Zugang Mao* and Susan B. Sinnott†

Department of Materials Science and Engineering, University of Florida, Gainesville, Florida 32611-6400

(Received 11 April 2002; published 20 December 2002)

The diffusive behavior of ethane and ethylene in single-walled carbon nanotubes is investigated using classical molecular dynamics simulations and density functional theory calculations. At low molecular densities, these nonspherical molecules follow a spiral path inside nanotubes with diameters of 13–22 Å, which maximizes the interaction of molecular C-C bonds with the C-C bonds in the nanotubes. Spherical molecules, such as methane, are not predicted to follow a spiral diffusion path. This result quantifies the manner in which molecular shape and chemical bonding affects molecule-nanotube interactions and indicates the generality of spherical transport through nanotubes.

DOI: 10.1103/PhysRevLett.89.278301 PACS numbers: 81.07.De, 02.70.Ns, 71.15.Mb, 81.07.Nb

The discovery of carbon nanotubes (CNTs) [1] over a decade ago has stimulated numerous studies of their unique properties [2–4]. CNTs can be defined as one or more seamless cylindrical sheets, or shells of graphite [5]. Because they have nanometer-scale diameters and a hollow, cylindrical shape, CNTs have been proposed as molecular sieves, nanoscale test tubes, hydraulic actuators, synthetic membranes, and selective adsorbents. There have been several studies of dynamic molecular flow [6–8], diffusive molecular flow [8,9], and molecular adsorption [10–13] in CNTs. There are also several reports on the introduction of metals and charged particles, such as iodine [14,15] and potassium [16] into nanotubes. In Ref. [15], the atomic static arrangement of iodine atoms inside single-walled CNTs was examined using both *Z*-contrast scanning transmission electron microscopy and density functional theory (DFT) calculations. Chains of iodine formed a double helix, spiral arrangement inside the CNTs. It was concluded that the chiral structure of the CNTs played an important role in this arrangement because of strong iodine-CNT interactions that resulted from the attraction of the charged iodine chains with the π electrons along the C-C bond directions in the CNT.

In this study, similarly strong interactions between nonspherical hydrocarbon molecules and CNTs are predicted to cause these molecules to follow a spiral diffusion path through the tubes under certain conditions. Classical molecular dynamics (MD) simulations with empirical potentials and first principles, DFT energy minimization calculations are used to make this prediction. The C-C bonds in small, nonspherical hydrocarbon molecules are predicted to align with the C-C bonds in the CNT walls for reasons similar to those proposed for iodine chains [15]. This finding quantifies the importance of molecular size, shape, and chemical bonding on molecular intercalation and transport through CNTs and has important implications for the use of CNTs as membranes and energy storage devices.

In the MD simulations, the forces on the atoms are calculated using empirical methods that vary with distance [8,9]. The short-range interactions are calculated using a many-body, reactive empirical bond-order hydrocarbon potential that realistically describes covalent bonding within both the organic molecules and CNTs [17]. The long-range interactions are characterized with a Lennard-Jones potential [8] that is only nonzero when the covalent empirical potential has gone to zero.

In the case of the first principles DFT calculations, the CASTEP program is used and the calculations utilize the local density approximation and the supercell approximation in combination with ultrasoft pseudopotentials and plane wave expansions [18,19]. The calculations use the density mixing technique to minimize the total energy with respect to plane wave coefficients, which use the Koelling-Harmon equation [20]. The pseudopotential plane wave kinetic energy cutoffs are 100 and 250 eV, and the convergence criteria are 0.000 005 eV/atom for energy and 0.05–0.1 eV/Å for the residual forces. Highly nonlocal exchange and correlation effects and van der Waals interactions far outside the nanotube walls are not included in these calculations.

Three molecules are considered in the MD simulations: two that are nonspherical (ethane and ethylene) and one that is spherical (methane). Zigzag and armchair single-walled CNTs are considered with diameters in the range 8–25 Å. The lengths of the nanotubes are 5–10 nm and both ends are open. The initial conditions and intermolecular potentials are identical to those described in Refs. [8,9]. Three temperatures are considered: 50, 150, and 300 K. During equilibration at the given temperature, the nanotube and 90% of the atoms in the system have Langevin frictional forces [21] applied to them. The total equilibration time is 1.5 ps. Following equilibration, all the atoms in the molecules are allowed to evolve with no constraints while the atoms in the nanotube walls continue to have Langevin frictional forces applied to them. This allows the CNT to mimic the energy-dissipation

properties of a μm-long nanotube when diffusing molecules collide with the tube walls. Time steps of 0.25 fs are used and most simulations run for 150 ps.

In molecular diffusion through CNTs, the balance between the interaction of the molecules and the nanotube walls and the intermolecular interactions among the molecules is important. As indicated in other studies [22], molecules can lower their energy by entering a CNT. However, in these nonequilibrium MD simulations, the density gradient is large and this causes the molecules, once they enter the nanotube, to move from the area of high molecular density to the area of low molecular density. The entropy of the system is also an important driving force, especially at higher temperatures. Under these conditions, the dynamic properties of the molecules will be slightly different over time. For this reason, the mean square averaging (MSA) technique is used to quantitatively analyze the molecular trajectories through the CNTs from the simulation results.

When the steady-state molecular density inside the CNT is low (around 0.145 g/cm^3 for ethylene and 0.156 g/cm^3 for ethane), almost all the ethane and ethylene molecules are predicted to follow a spiral diffusion path inside CNTs with diameters of 13–22 Å, as determined from the MSA technique and visualization of the trajectories in movies. The molecules line up their C-C bonds with the C-C bonds in the tube wall and then diffuse along the length of the CNT following the path of lowest potential energy. This path maintains the C-C bond alignment between the molecule and the CNT wall and therefore is related to the chirality of the CNT, as shown in Fig. 1. Methane is not predicted to follow a spiral diffusion path because it is not able to get close enough to the tube wall to interact strongly with the C-C bonds there. Rather, methane diffuses down the center of the CNTs, as discussed in [8].

At steady-state molecular densities of about 0.386 g/cm^3 for ethylene and 0.408 g/cm^3 for ethane inside the tubes, the spiral path is only predicted to occur for the first 3–8 molecules that enter the CNT. As more molecules enter the nanotube, the molecular density increases to its steady-state value and some molecules move to the center of the tube to maximize their interactions with each other, which increases the amount of disorder in the system. The energy of the system is lowered more from these intermolecular interactions than is gained from maintaining the C-C bond alignment between the molecules and the CNT wall.

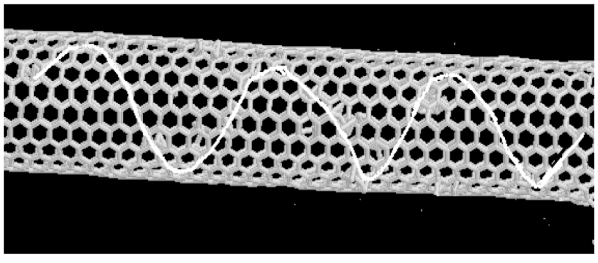

FIG. 1. The line represents the averaged path followed by 18 ethane molecules diffusing through a (10,10) CNT at 300 K in the MD simulation trajectories.

When the diameter of the CNT is less that 13 Å, the curvature of the CNT is so great that the ethane and ethylene molecules cannot get close enough to the tube wall to follow a spiral path. Instead, they are forced into the center of the CNT. When the diameter of the CNT is greater than 25 Å, the curvature is low, which results in a weakened CNT-molecule interaction and more significant molecule-molecule interaction. Although many molecules still prefer to diffuse along the CNT walls, the trajectory of motion of the molecules is random rather than along well-defined spiral paths. This randomness of motion also means that a significant number of molecules occupy the center of the nanotube, rather than staying close to the walls all the time. Similarly, no orientational diffusion is seen on graphite because the strength of the interaction energy between the molecules and graphite surface is too low.

Zigzag and armchair CNTs of similar diameters are considered in this study, as shown in Table I. There is a consistent, small difference in the diffusion path followed by ethane and ethylene in all the CNTs considered because the C-C double bond of ethylene lines up with the C-C bonds in the walls more easily than the C-C single bond of ethane. The distance between the molecules and the CNT wall in armchair tubes is larger than in zigzag tubes because the angle between the molecular axis and the nanotube axis is different in the two types of CNTs. For example, the MD simulations predict that the molecules arrange themselves so that their angle relative to the CNT axis is 44.3° in (10,10) CNTs and 31.5° in (19,0) CNTs at 300 K. This is because of the differing arrangement of C-C bonds in zigzag and

TABLE I. The spiral path of ethane and ethylene molecules inside CNTs at 300 K. The spiral diameter is defined as the diameter of the spiral molecular trajectory along the cross section of the CNTs, and z is the distance traveled by the molecules along the nanotube axis when a molecule completes one spiral.

Type of nanotube (Diameter)	Spiral diameter $2H$ (Å)		Distance z (Å)	
	Ethane	Ethylene	Ethane	Ethylene
(17,0) (13.5 Å)	7.7	7.8	33.5	31.8
(21,0) (16.7 Å)	11.2	11.3	48.9	46.5
(24,0) (19.1 Å)	14.0	14.1	67.1	64.4
(28,0)(22.2 Å)	17.7	17.9	78.3	77.2
(10,10) (13.75 Å)	7.4	7.6	23.1	21.6
(12,12) (16.5 Å)	10.6	10.7	33.6	32.1
(14,14) (19.25 Å)	13.1	13.2	45.8	44.7
(16,16) (22.1 Å)	16.7	16.9	56.2	55.3

armchair CNTs; one complete spiral covers more distance down the tube axis in one than in the other.

Similar spiral paths of molecular motion of ethane and ethylene in (10,10) and (19,0) CNTs are predicted at all three temperatures considered. As the temperature decreases from 300 to 50 K, the molecules move slightly closer to the tube walls and follow a more perfect spiral path because they have less randomizing thermal energy. In all cases, the spiral path followed by the nonspherical molecules can be quantitatively expressed as

$$K = x\boldsymbol{i} + y\boldsymbol{j} + z\boldsymbol{k}, \tag{1}$$

where $\boldsymbol{i}$, $\boldsymbol{j}$, and $\boldsymbol{k}$ are the three-dimensional unit vectors of the CNTs, with $\boldsymbol{i}$ and $\boldsymbol{j}$ representing normal vectors in the cross section of the CNTs, $\boldsymbol{k}$ representing the direction of the CNT axis, z representing the distance traveled down the CNT axis, and x and y representing the molecular spiral parameters related to the interaction between the CNTs and the molecules, the degree of molecular linearity, and the chirality of the CNTs. For ethane and ethylene, x and y can be written as

$$x = H\sin(2\pi\alpha t^m), \tag{2}$$

$$y = H\cos(2\pi\alpha t^m), \tag{3}$$

where H is a spiral coefficient that is equal to the spiral radius of the CNT, α is a coefficient related to the diffusion coefficient and the helical structure of the CNT, m is the structure index that is related to the diffusion mode and is equal to $\frac{1}{2}$ in the simulations, and t is time. The average distance traveled by each molecule, z, is [8,9]

$$z^2 = 2Ct^n, \tag{4}$$

where C is the mobility or diffusion coefficient (depending on the diffusion mode) and n varies from $\frac{1}{2}$ for single-file mode diffusion to 1 for normal-mode diffusion.

In this work, if the helical structure of the CNTs is expressed as (a, b) [5], H can be written as

$$H = \frac{a}{2(a + 0.05b)}[D - 2\lambda - d(D_0/D)], \tag{5}$$

where λ is the effective π bond length of the nanotube walls (which is 1.7 Å), D_0 is the cutoff diameter of the CNTs below which the molecules can only stay in the middle of CNTs (which is 8.0 Å for ethane and ethylene), D is the diameter of the CNT, and d is the effective size of molecules (which is 3.99 Å for ethane and 3.93 Å for ethylene [9]). The factor of 0.05 in the denominator of Eq. (5) was obtained from linear regression analysis of the simulation results. The coefficient α is

$$\alpha = \sqrt{\frac{C}{2H^2}}\frac{a + b}{2a}. \tag{6}$$

Ethane and ethylene only follow spiral diffusion paths when they diffuse through normal mode diffusion [when the value of n in Eq. (4) is 1]. The values C, α, and H are given in Table II for the systems considered. When the molecules follow single-file diffusion or diffusion modes that are transitional between single file and normal mode [8], the ethane and ethylene molecules are in the center of the CNTs, rather than close to the walls. Therefore, no spiral diffusion is predicted to occur for these diffusion modes. Thus, the simulations predict that the spiral path followed by the molecules is strongly dependent on the diffusion mode of the organic molecules and the helical structure of CNTs. Both left-handed and right-handed spiral paths are detected in the simulations. The handiness of the spiral path followed by a particular molecule varies with the relaxation state of the molecule and the system.

Self-consistent, first-principles, DFT calculations are used to check the results of the MD simulations. These conditions are similar to those in [23], where H_2 desorption from Al(110) surfaces was examined. Two similarly sized CNTs of differing chirality are considered: a (10,10) armchair CNT with a 13.75 Å diameter and a (19,0) zigzag CNT with a 15.08 Å diameter. The calculations consider only half of the tube (a hemisphere) as was done in Ref. [15]. The energy-minimized structure of the ethane molecules at different angle orientations from (from 0° to 90°) along each nanotube axis is examined. The distance between the molecules and the CNT walls is

TABLE II. Diffusion coefficient, C, of molecules diffusing through different CNTs found by fitting the averaged distance traveled by the molecules in time to Eq. (4). The value of n in Eq. (4) is 1. The parameters for α and H are given for Eqs. (5) and (6).

Type of tubes (a, b) (Diameter of tubes)	Ethane			Ethylene		
	C (cm^2/s)	α	H	C (cm^2/s)	α	H
(17,0) (13.5 Å)	1.04×10^{-4}	9.42×10^{-4}	3.82	9.28×10^{-5}	9.38×10^{-4}	3.86
(21,0) (16.7 Å)	4.82×10^{-5}	4.34×10^{-4}	5.64	3.75×10^{-5}	4.32×10^{-4}	5.68
(24,0) (19.1 Å)	1.94×10^{-5}	2.23×10^{-4}	6.97	1.36×10^{-5}	2.22×10^{-4}	7.00
(28,0) (22.2 Å)	7.95×10^{-6}	1.15×10^{-4}	8.63	6.89×10^{-6}	1.15×10^{-4}	8.66
(10,10) (13.75 Å)	9.88×10^{-5}	1.85×10^{-3}	3.78	9.20×10^{-5}	1.85×10^{-3}	3.80
(12,12) (16.5 Å)	5.02×10^{-5}	9.49×10^{-4}	5.27	4.14×10^{-5}	9.47×10^{-4}	5.30
(14,14) (19.25 Å)	1.78×10^{-5}	4.44×10^{-4}	6.73	1.25×10^{-5}	4.43×10^{-4}	6.75
(16,16) (22.1 Å)	8.24×10^{-6}	2.48×10^{-4}	8.30	6.98×10^{-5}	2.48×10^{-4}	8.32

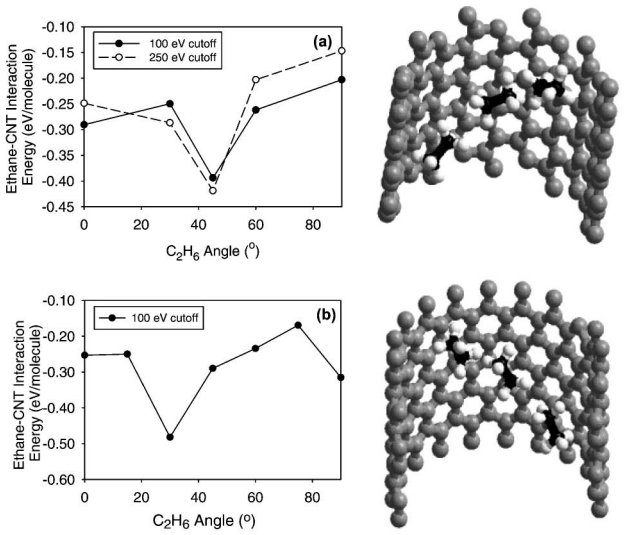

FIG. 2. Molecule-CNT interaction energies and shapshots from the DFT calculations of ethane molecules oriented along the axis of (a) a (10,10) CNT at kinetic energy cutoffs of 100 and 250 eV and (b) a (19,0) CNT at a kinetic cutoff of 100 eV. The energies are for the ethane in various orientations while the snapshots show the optimal configurations predicted by the DFT calculations. The distance between the molecule and the nanotube wall is 0.35–0.45 nm.

optimized at each orientation using the Broyden-Fletcher-Goldfarb-Shanno Hessian update method [24], and the ethane-CNT interaction energy is calculated for each configuration.

Figure 2 plots the interaction energies between the ethane molecules and the tube walls at each optimized position for the various orientations along each CNT axis. In the case of the armchair tube, the ethane-CNT interaction energy varies from -0.20 to -0.39 eV for cutoff energies of 100 eV, and -0.15 to -0.42 eV for cutoff energies of 250 eV, with the lowest energy occurring at 45° on the CNT axis in each case. In the case of the zigzag tube, the ethane-CNT interaction varies from -0.17 to -0.48 eV, with the lowest energy occurring at 30° on the CNT axis. Hence, the DFT calculations confirm that nonspherical organic molecules such as ethane strongly prefer specific orientations inside CNTs, and that these orientations are related to the CNT's helical structures. The angle preferences found in the DFT calculations are in excellent agreement with the molecular motion paths predicted in the MD simulations. Specifically, the MD simulations predict an angle of 44.8° (44.3°) for spiral motion along the axis in the (10,10) CNT and an angle of 30.7° (31.5°) for spiral motion along the axis in the (19,0) CNT at 50 K (300 K). Figure 2 also shows snapshots of the optimal diffusion path of ethane in (10,10) and (19,0) CNTs from the DFT calculations, which illustrate how the spiral path is different in each CNT because of their differing chiralities.

In conclusion, our simulations and first principles calculations have quantified the level of alignment of C-C bonds in small, nonspherical hydrocarbon molecules with C-C bonds in CNT walls that maximizes molecular-CNT interactions. The alignment is found to be strong enough that the affected molecules diffuse along a spiral path down the CNT axis under appropriate conditions.

The authors gratefully acknowledge support of this work by the NASA Ames Research Center and the Advanced Carbon Materials Center at the University of Kentucky, and the assistance of Douglas Irving in performing some of the calculations.

*Current address: Department of Materials Science and Engineering, Northwestern University, Evanston, Illinois 60202.
†Author to whom correspondence should be addressed. Electronic address: sinnott@mse.ufl.edu

[1] S. Iijima, Nature (London) **354**, 56 (1991).
[2] J.W. Mintmire, B. I. Dunlap, and C. T. White, Phys. Rev. Lett. **68**, 631 (1992).
[3] R. S. Ruoff and D. C. Lorents, Carbon **33**, 925 (1995).
[4] T.W. Ebbesen, J. Phys. Chem. Solids **57**, 951 (1996).
[5] M. S. Dresselhaus, G. Dresselhaus, and P. C. Eklund, *Science of Fullerenes and Carbon Nanotubes* (Academic, San Diego, 1996).
[6] R. E. Tuzun *et al.*, Nanotechnology **7**, 241 (1996).
[7] R. E. Tuzun *et al.*, Nanotechnology **8**, 112 (1997).
[8] Z. Mao and S. B. Sinnott, J. Phys. Chem. B **104**, 4618 (2000).
[9] Z. Mao and S. B. Sinnott, J. Phys. Chem. B **105**, 6916 (2001).
[10] M. Muris *et al.*, Langmuir **16**, 7019 (2000).
[11] M.W. Cole *et al.*, Phys. Rev. Lett. **84**, 3883 (2000).
[12] J. Hilding *et al.*, Langmuir **17**, 7540 (2001).
[13] T. D. Power, A. I. Skoulidas, and D. S. Sholl, J. Am. Chem. Soc. (to be published).
[14] L. Grigorian *et al.*, Phys. Rev. B **58**, R4195 (1998).
[15] X. Fan *et al.*, Phys. Rev. Lett. **84**, 4621 (2000).
[16] G. Gao, T. Cagin, and W. A. Goddard III, Nanotechnology **9**, 184 (1998).
[17] D.W. Brenner *et al.*, J. Phys. Condens. Matter **14**, 783 (2002).
[18] M. C. Payne *et al.*, Rev. Mod. Phys. **64**, 1045 (1992).
[19] V. Milman *et al.*, Int. J. Quantum Chem. **77**, 895 (2000).
[20] D. Vanderbilt, Phys. Rev. B **41**, 7892 (1990).
[21] M. P. Allen and D. J. Tildesley, *Computer Simulation of Liquids* (Oxford University Press, New York, 1987).
[22] M. R. Pederson and J. Q. Broughton, Phys. Rev. Lett. **69**, 2689 (1992).
[23] B. Hammer *et al.*, Phys. Rev. Lett. **69**, 1971 (1992).
[24] W. H. Press *et al.*, *Numerical Recipes: The Art of Scientific Computing* (Cambridge University Press, Cambridge, England, 1989).